DEVELOPMENT OF A DEEP LEARNING NEURAL
NETWORK MODEL FOR TRANSIENT AND SMALL
SIGNAL STABILITY ASSESSMENT

John Obiajulu Onyemenam
Department of Electrical and Information Engineering,
Landmark University, Omu-Aran, Nigeria
john.obiajulu@lmu.edu.ng

Paul Kehinde Olulope
Department of Electrical and Information Engineering,
Ekiti State University, Nigeria
paulade001@yahoo.com

Nnaemeka Uchenna Okeke
Department of Electrical and Information Engineering,
Landmark University, Omu-Aran, Nigeria
okeke.uchenna@lmu.edu.ng

Emmanuel Osaji
Department of Electrical and Information Engineering,
Landmark University, Omu-Aran, Nigeria
osaji.emmanuel@gmail.com

ABSTRACT

This paper suggests employing a deep learning neural network (DLNN) technique to evaluate both small signal and transient stability, in contrast to earlier studies that focused only on transient stability. The complexity of power system dynamic features has increased due to the introduction of new components like power electronics, electric vehicles, and renewable energy generation, making TSA and SSA essential considerations. Today, the stability and security of the electrical network are impacted by the growing development of renewable energy sources. Wide area monitoring systems for the electrical system have emerged, creating "big data," which has ushered in new paradigms for tackling these issues. A wide range of stakeholders are paying attention to transient stability and small signal stability issues because they have the potential to create catastrophic outages. This study's objective is to evaluate the numerous stability issues relating to the electrical system using feature selection and DLNN methodology. The 28-bus test case power system's dynamic simulations were used to provide Nigerian time-domain data. A data processing pipeline for feature selection is built using the Relief-F feature selection approach. If a system is transiently stable, the prediction model will advise the power system operator of the damping of low frequency local and inter-area oscillations. The DLNN approach also provides information on the system's oscillatory dynamic response and

transient stability, enabling the application of essential control measures. Calculations are made to determine the proper amount of adjustment, the correct minimum damping ratio, and system stability under the constraints of stability and power balance. The DIgSILENT/Python tool, which is powered by an Intel Pentium core i5 2GHz CPU, is used to carry out this study. The Nigeria 28 bus system is used to test the suggested model's higher performance, and the IEEE 9 bus system is used to confirm it. The accuracy performance of Nigeria's 28 bus system was evaluated at 90.16 percent for TSA and 100 percent for SSA. This study assesses and confirms the viability of the suggested model.

Keywords- Small Signal stability assessment, Transient stability assessment, Deep Learning Neural Network, Long-short Term Memory, Transient stability, Power system stability, Relief F, Recurrent Neural Network

I. INTRODUCTION

Power system stability refers to a power system's ability to recover from a disruption, reach equilibrium, and resume normal operations. Rotor angle instability brought on by synchronism loss has long been linked to the instability issue [7]. Rotor angle stability can also be split into small signal and large signal stability depending on the strength of the disturbance. Because of this, tiny signal and transient stability, respectively, refers to a power system's capacity to sustain synchronism in the face of small and substantial disruptions [2]. The behavior of synchronous generators in relation to their associated control systems, loads, renewable energy production, flexible AC transmission devices (FACTs), and the transmission network is described by a set of highly nonlinear Differential and Algebraic Equations (DAE) [2] and [7]. When a power system undergoes minor modifications, the DAE model can be linearized all the way around the equilibrium point. Electrical torque variations in synchronous machines with the appropriate synchronizing and dampening torque component enable small-signal stability. However, when a power system experiences significant changes, the DAE model cannot be linearized around an operational point; as a result, it must be numerically solved for each situation using time domain simulations [7]. If there is inadequate synchronizing and damping torque, the rotor angle of a synchronous generator may occasionally drift and oscillate [2]. Power outages are mostly caused by transient instability, which can also lower a power system's overall performance [4]. Time domain simulations, a sort of TSA, are costly and computationally challenging, especially for big power systems with a nearly infinite number of operating points and contingencies. To achieve these objectives, the prediction model is trained using a Deep learning technique (LSTM) and a data set for a range of operating conditions. The considerable weekly damped low frequency oscillation is gradually captured by the Long Short Term Memory (LSTM), which is trained to remember the oscillatory response of a projected stable system. By reducing the TSA and SSA's computational complexity over time, the LSTM improves prediction accuracy even further. The Nigeria 28 Bus System is used to demonstrate the suggested model's improved performance, and the IEEE 9 Bus system is used to corroborate it.

II. TRANSIENT AND SMALL SIGNAL STABILITY OF A POWER SYSTEM

In this research, a prediction model for the Transient and Small Signal Stability Problems in Nigeria's 28 bus system is constructed using deep learning neural network methodologies. The mathematical process for transient and small signal stability is described in this section.

A. Transient Stability

Rotor angle stability is a term used to describe a synchronous machine's capacity to sustain synchronism in a power system following an interruption. Because power system disturbances do not always have the same consequences on generation, certain generators will experience additional load as a result of adaptive operation and will slow down, while the remaining generators will raise their speed to maintain grid frequency. Rising generator speed causes a shift in the rotor's tilt in relation to the stator [6]. To maintain balance between the mechanical input torque and the electrical output torque, the rotor alternates between accelerating and decelerating continually. This behavior reduces the generator's capacity to generate electricity and damages the generator, prime mover, and transformers. Therefore, it is necessary to secure the synchronous machine [8].

The dynamic reaction of a power system to disturbances is controlled by a collection of DAE, and their compact form is:

$$x = h\,(x, y) \qquad\qquad (1)$$

$$0 = g\,(x, y) \qquad\qquad (2)$$

Indicated are the state and algebraic variables x and y. Additionally, the vectors of the pertinent DAE are shown by h and g. The algebraic variables y, such as bus voltages and active power injections, and the state variables x, such as rotor angles and frequencies, are solved to get time-varying trajectories. Numerical techniques, such as the trapezoidal approach equation (1), are used to discretize the set of differential equations in order to achieve this. The generated algebraic equations and the remaining algebraic equations are solved by the Newton's technique at each time step (2). To evaluate transient stability, the dynamic trajectories over the simulation time window are monitored. This method provides an accurate assessment of temporary for a specific situation [1].

B. Small signal stability

Inadequate oscillation damping in frequency, rotor angle, or voltage stability indicators are signs of small signal stability. When damping is zero, oscillatory activity's amplitude remains constant across time. Independent of the initial disturbance, negative damping increases the amplitude of the oscillations. High damping ratios increase the critical mode of the power system, which reduces oscillation behavior. this is due to the fact that it represents the system's least stable component [7]. The stability of tiny signals can be examined using the smallest damping ratio. Small signal stability issues might be local or global in nature. Local mode oscillations are smaller disturbances caused by a single producing station while interarea mode oscillations are larger disturbances caused by a group of generating

stations. In order to increase oscillation stability in multiple-machine power systems, Power System Stabilizer (PSS) and Flexible AC Transmission System (FACTS) controllers are frequently employed. These devices lessen damping by creating additional signals to counter oscillations in generator excitation systems [5] and [7]. The electrical torque of synchronous machines is the most important variable in determining how they react to oscillations. Electrical torque is made up of the Synchronizing Torque (TS), which is in phase with the rotor angle deviation during an oscillation event, and the Damping Torque (TD), which is in phase with the speed deviation components. Both kinds of torques have an effect on the stability of tiny signals [5]. The set of algebraic and differential equations stated in (1) - (2) can be linearized around an equilibrium point for mild disturbances, as shown in equations (3) - (4).

$$\Delta x = A\Delta x + B\Delta y \qquad (3)$$

$$0 = C\Delta x + D\Delta y \qquad (4)$$

$$A = \frac{\partial h}{\partial x}, B = \frac{\partial h}{\partial x}, C = \frac{\partial h}{\partial x}, D = \frac{\partial h}{\partial x} \quad (5)$$

The linearized model in (3) - (4) is used to examine minor signal or local stability at an equilibrium point in the presence of a small disturbance in a power system. The Lyapunov first technique is used to achieve this, and it includes figuring out the eigenvalues of the characteristic equation as follows [3].

$$\det(A_{sys} - \lambda I) = 0 \qquad (6)$$

Where, $A_{sys=A-B\,(D^{-1})C}$ and $\lambda = (\lambda 1,\ \lambda 2 \ldots\ldots\ldots\ldots\ldots\ldots\ldots\ldots\ldots\ldots\lambda n)$

Either real or complex estimated eigenvalues result in non-oscillatory or oscillatory responses. Additionally, conjugate pairs of complex eigenvalues are present, each of which indicates an oscillatory mode [5].

C. LONG SHORT TERM MEMORY NETWORK FOR TSA AND SSA

LSTM networks are RNN versions that may retrieve information from the past in time series data. The network learns by encoding incremental time domain inputs into durable internal hidden states. The practice of recalling prior knowledge over time is common. Since LSTMs are capable of remembering previous inputs, they are useful for time-series prediction [7]. LSTMs, which have a chain-like structure and four interacting layers, interact in various ways. In addition to time-series predictions, LSTMs are frequently used in speech recognition, music production, and pharmaceutical research [7] and [10]. The issues with the long-term dependency problem are dealt with using LSTM. LSTM includes the option to read, write, or reset the sale at each stage [10]. The mathematical calculations for the LSTM are shown in Equation 7.

$$i_t = \sigma\left(W_{ih}h_{t-1} + W_{ix}X_t + b_i\right),$$
$$\hat{c}_t = \tanh(W_{\hat{c}h}h_{t-1} + W_{cx}X_t + b_c),$$
$$c_t = c_{t-1} + i_t.\hat{c}_t, \qquad\qquad (7)$$
$$0_t = \sigma\left(W_{oh}h_{t-1} + W_{ox}X_t + b_o\right),$$
$$h_t = 0_t.\tanh(c_t),$$

The operator denotes the pointwise multiplication of two vectors, where ct stands for the state of the LSTM cell, and Wi, Wc, and Wo are the weights. The input gate selects what fresh information can be entered while updating the cell state, while the output gate selects what information can be output based on the cell state. The LSTM cell shown in equation 8 can be mathematically characterized as follows based on the connections:

$$f_t = \sigma\left(W_{fh}h_{t-1} + W_{fx}X_t + b_f\right),$$
$$i_t = \sigma\left(W_{ih}h_{t-1} + W_{ix}X_t + b_i\right),$$
$$\hat{c}_t = \tanh(W_{ch}h_{t-1} + W_{ix}X_t + b_{\hat{c}}),$$
$$c_t = f_t.c_{t-1} + i_t.\hat{c}_t, \qquad\qquad (8)$$
$$o_t = \sigma\left(W_{oh}h_{t-1} + W_{ox}X_t + b_o\right),$$
$$h_t = o_t.\tanh(c_t).$$

The forget gate determines which information from the cell state will be deleted. This information is stored when the forget gate, ft, has a value of 1, and it is completely discarded when it has a value of 0 [10]. The LSTM's structure is depicted in Figure 1.
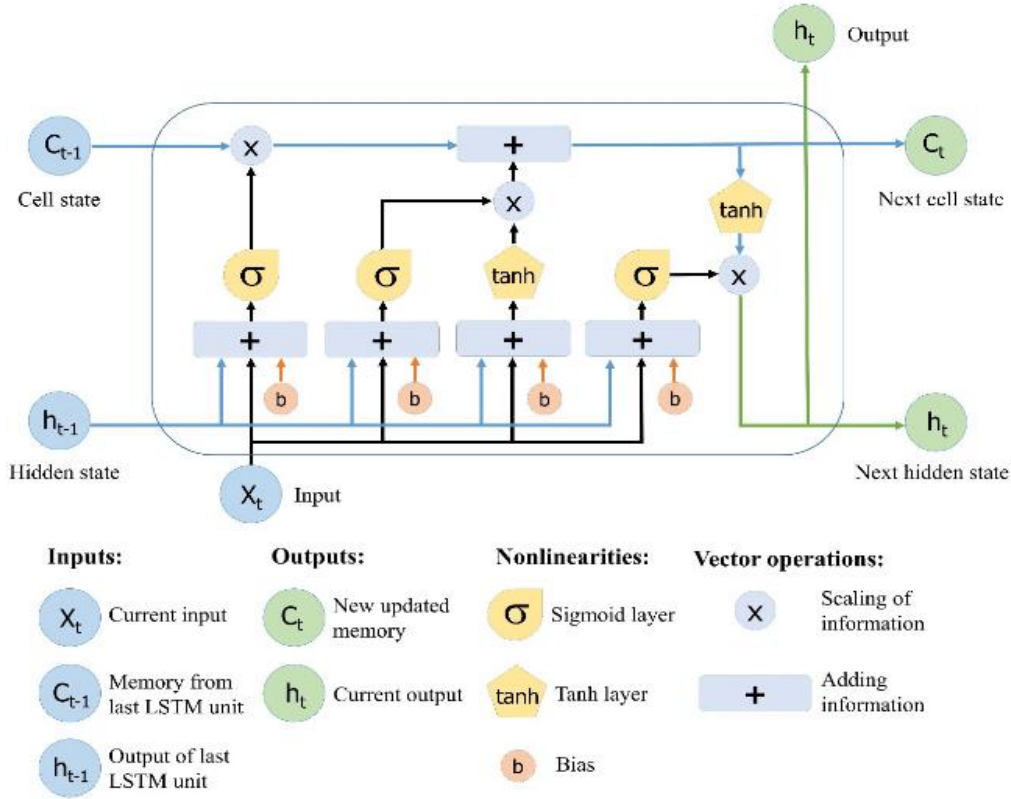
Figure 1: LSTM Network Diagram [11].

III. NETWORK STRUCTURE OF THE MODEL

In order to create a Deep learning NN for TSA and SSA, this paper builds the six-layer network model are explained below

    i.   Data collection: The National Control Center (NCC), Oshogbo, is where appropriate data for modeling the 28-bus Nigeria network are acquired.

    ii.   Using DIgSLIENT, the Nigeria 28 bus system was network modeled.

    iii.   Data collection for DLNN: The Relief-F technique is applied to remove irrelevant data from redundant ones.

    iv.   DLNN (LSTM): To perform the necessary TSA and SSA evaluation, a DLNN based on LSTM is modelled based on the data that is available, trained, tested, and verified.

    v.   Performance evaluation: The Root Mean Squared (RMS), Specificity, Accuracy, and Precision measures are then used to evaluate the performance of the LSTM model.

    vi.   Compare outcomes: The outcomes are evaluated against the IEEE 9 bus system.

Figure 2, shows the proposed model for assessing Transient and Small signal stability. It is made up of two different model. The two model contains four inputs namely, voltage, rotor angle, active power and reactive power.
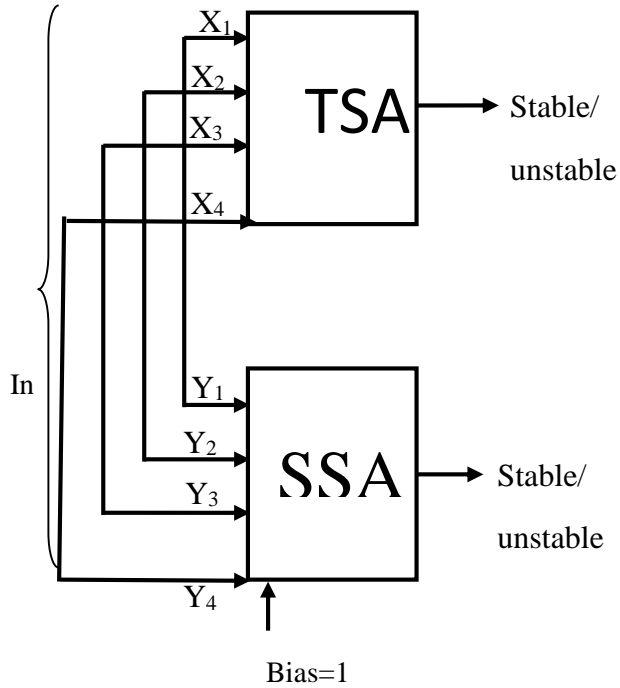

Figure 2: Schematic design model of TSA & SSA

IV. DATA PREPARATION

The 330KV, 28 bus network in Nigeria that was used as the case study (TCN) was furnished with the bus and transmission line data by the National Control Center (NCC). The 28-bus power network, which includes 28 buses, 9 generation stations, and 52 transmission lines, is shown in Figure 3. The bus data and transmission line are shown in Table 1. The DIgSILENT power factory is where the modeling is done. According to where the load and generator were located, the bus bars were either modelled as PV or PQ when it came to the transmission lines. The loads were PQ data-based lumped loads. The generators were accurately modeled using the necessary data and synchronous generator characteristics.
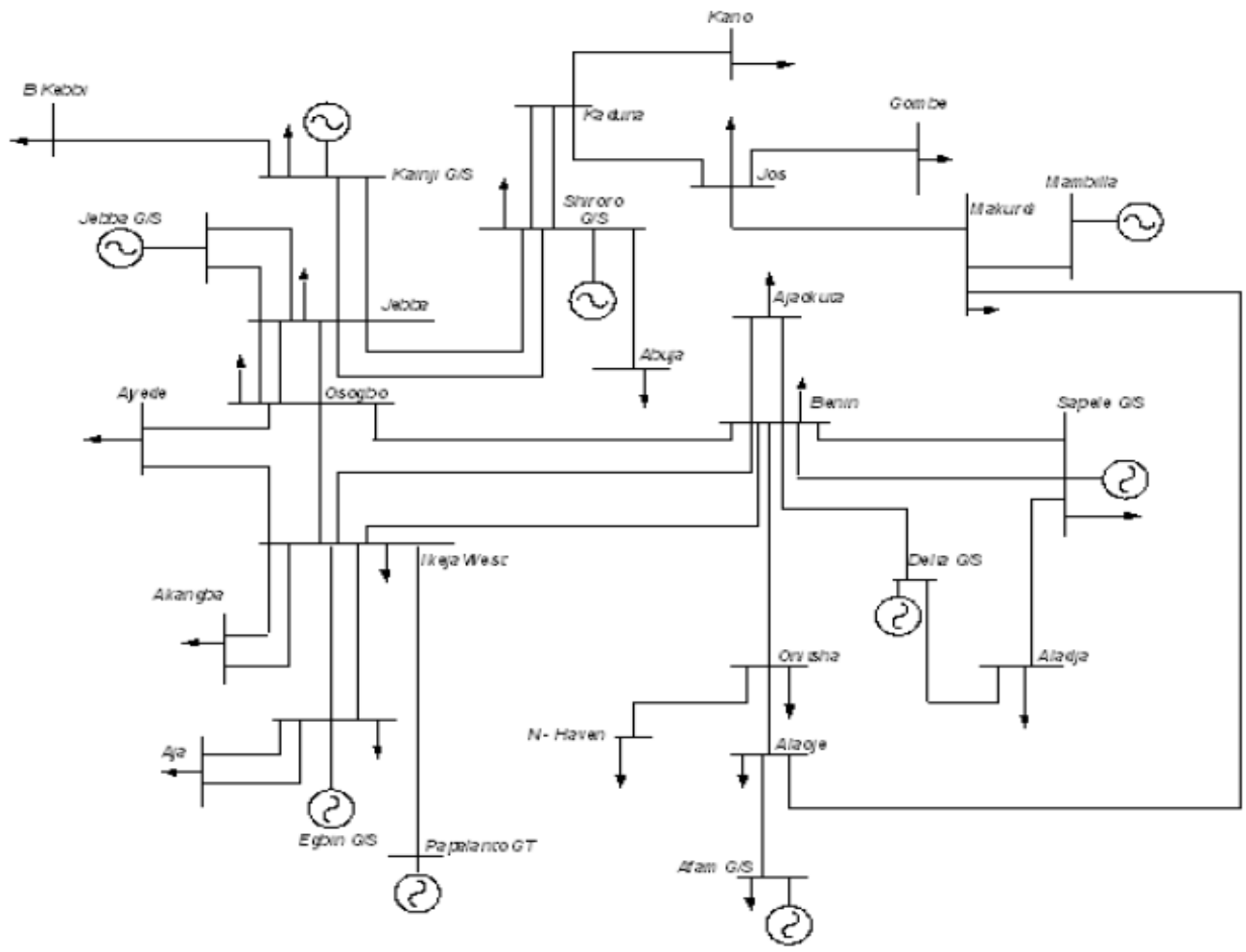
Figure 3: The Nigerian 28 bus power system [9].

Table 1: Network Data of the Nigerian 28 Bus Power System [9].

Bus Identification		Bus Loads		Transmission Lines Data			
NO	Name	MW	MVAR	Bus		R(pu)	X(pu)
				FROM	TO		
1	Egbin	68.90	51.70				
2	Delta	0.00	0.00	1	3	0.0006	0.0044
3	Aja	274.40	205.80	4	5	0.0007	0.0050
4	Akangba	244.70	258.50	1	5	0.0023	0.0176
5	Ikeja-West	633.20	474.90	5	8	0.0110	0.0828
6	Ajaokuta	13.80	10.30	5	9	0.0054	0.0405
7	Aladja	96.50	72.40	5	10	0.0099	0.0745
8	Benin	383.30	287.50	6	8	0.0077	0.0576
9	Ayede	275.80	206.8	2	8	0.0043	0.0317
10	Osogbo	201.20	150.90	2	7	0.0012	0.0089
11	Afani	52.50	39.40	7	24	0.0025	0.0186
12	Alaoji	427.00	320.20	8	14	0.0054	0.0405
13	New-Heaven	177.90	133.40	8	10	0.0098	0.0742
14	Onitsha	184.60	138.40	8	24	0.0020	0.0148
15	B/Kebbi	114.50	85.90	9	10	0.0045	0.0340
16	Gombe	130.60	97.90	15	21	0.0122	0.0916
17	Jebba	11.00	8.20	10	17	0.0061	0.0461
18	Jebba G	0.00	0.00	11	12	0.0010	0.0074
19	Jos	70.30	52.70	12	14	0.0060	0.0455
20	Kaduna	193.00	144.70	13	14	0.0036	0.0272
21	Kanji	7.00	5.20	16	19	0.0118	0.0887
22	Kano	220.60	142.90	17	18	0.0002	0.0020
23	Shiroro	70.30	36.10	17	23	0.0095	0.0271
24	Sapele	20.60	15.40	17	21	0.0032	0.0239
25	Abuja	110.00	89.00	19	20	0.0081	0.0609
26	Makurdi	290.10	145.00	20	22	0.0090	0.0680
27	Mambila	0.00	0.00	20	23	0.0038	0.0284
28	Papalanto	0.00	0.00	23	25	0.0038	0.0284
				12	26	0.0071	0.0532
				19	26	0.0059	0.0443
				26	27	0.0079	0.0591
				5	28	0.0016	0.0118

V. RESULT AND DISCUSSION

The LSTM and Relief-f algorithm are used to conduct the test. In this study, Python/DIgSLIENT is used to implement the study. Figure 4 below shows DIgSILENT model of Nigeria 28-bus power system for TSA and SSA. Data were obtained from DIgSILENT under different contingencies for TSA and SSA.
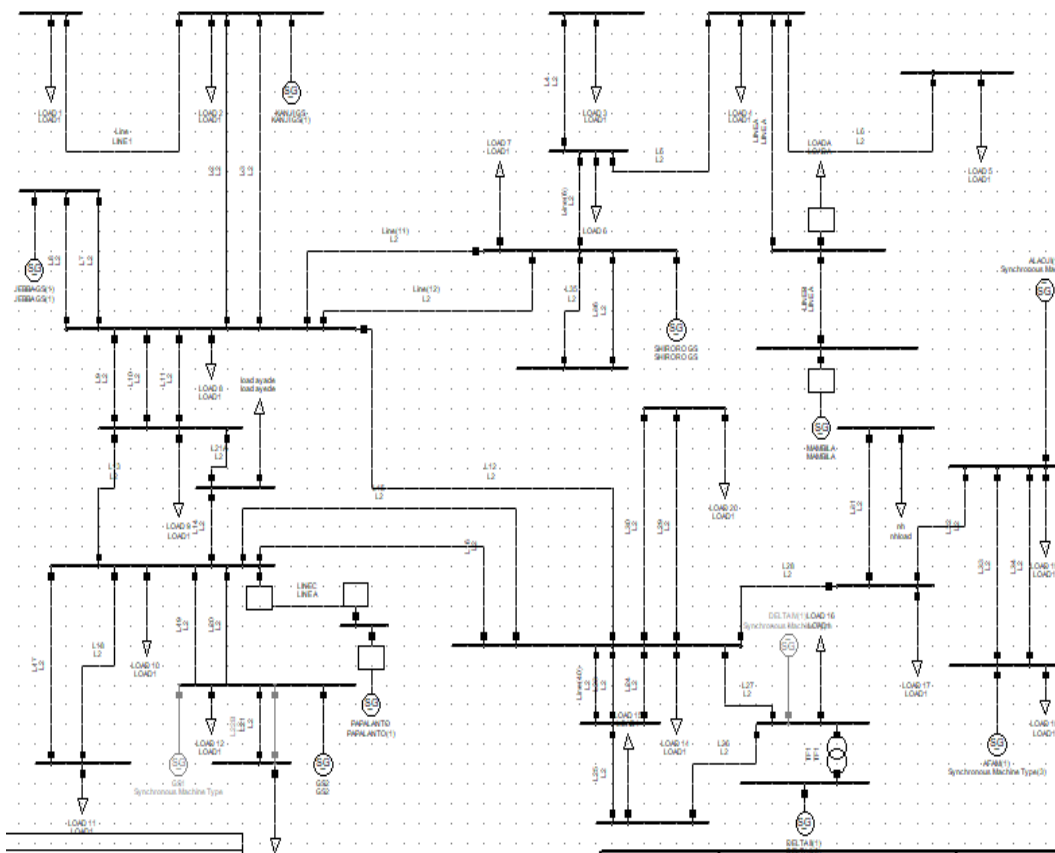

Figure 4: Modelling of Nigerian 28-Bus System

In this study the user interface gives user the privilege to load dataset, select relevant information from the huge amount of data, using the Relief-F feature selection algorithm, it helps preprocess and selects relevant subset of the data. Table 2 shows the loaded data.

Table 2: Loaded Data Nigerian 28-Bus System

V(p.u)	P(KW)	Q (KVAr	δ(Θ)	TSA Targ	SSA Targ
0.388583	-271.618	0.454232	-63.3957	0	1
0.469965	563.2468	-306.641	97.48929	0	1
0.255932	-209.335	151.7141	-102.012	0	1
0.533196	409.5992	-385.232	58.1159	0	1
0.147646	19.65125	190.0627	-142.138	0	1
0.540542	127.6128	-338.973	17.22918	0	1
0.220532	318.4933	72.08323	176.2186	0	1
0.484492	-151.327	-180.955	-25.1795	0	1
0.370508	535.4349	-148.529	133.0507	0	1
0.366197	-274.478	26.74668	-69.1091	0	1
0.489727	539.7334	-341.938	88.36538	0	1
0.209501	-156.153	174.4907	-114.545	0	1
0.543035	309.6819	-389.185	42.17829	0	1
0.154649	150.4527	153.4337	-161.475	0	1
0.514599	-27.5849	-260.075	-5.50633	0	1
0.310105	458.6298	-49.8561	150.0938	0	1
0.403731	-252.811	-30.6135	-54.6958	0	1
0.465345	553.8266	-304.05	100.1514	0	1
0.233219	-197.255	154.0606	-105.39	0	0.135
0.54455	350.7548	-412.666	48.70475	0	0.135
0.261644	-207.228	163.5346	-100.006	1	1
0.533944	476.4872	-393.262	69.36015	1	1
0.18805	-114.21	196.6741	-121.668	1	1
0.558244	357.5287	-423.106	46.91436	1	1
0.143834	28.34095	192.7953	-144.893	1	1
0.557052	193.1078	-381.217	22.91489	1	1
0.174444	207.5377	142.6571	-169.663	1	1
0.529761	5.899559	-279.595	-2.62709	1	1

In this study, the loaded data is preprocessed, analyzed using Relief-f with DLNN, the loaded data, comprises of 81,802 instances and 6 attrbutes, in the attribute, there are two targets stated as Stable/Unstable and Eigen value. The

loaded data is preprocessed using Relief-F, the selected or relevant feature is passed into DLNN. DLNN comprises of input layers, hiden layers and output using the LSTM. Figure 5 shows the ANN Fitting view for the data.
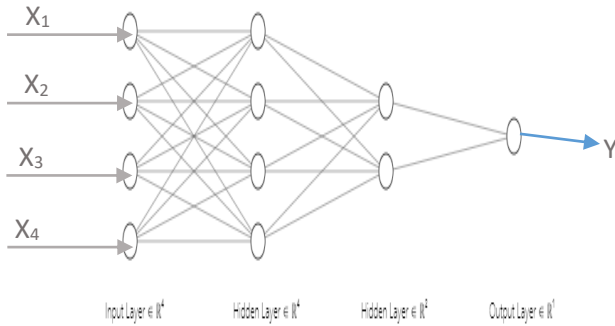

Figure 5: Fitting Layers of the Data

The output of TSA and SSA is either stable or unstable. For TSA when a system is stable is denoted as 1 and for an unstable system is denoted as 0. In contrast, for SSA, if the real part of the eigenvalue is negative and the damping ratio is positive, the system is stable or oscillatory free but, if the real part of the eigenvalue is positive, the system is unstable.Table 3 shows, the deep learning neural network artictecthure of TSA and SSA.

Table 3: Deep learning Neural Network Data and Structure of TSA & SSA

Feature And Structure Of LSTM	TSA AND SSA
Number of inputs	4
Number of neurons in the hidden layer	6
Output	1 each
Training data	66560
Testing data	8256
Validation data	6273
Training algorithm	LSTM
Epoch	31
Transfer function	Relu and Sigmoid

Figure 6 depicts the model confusion matrix used to calculate the created model's evaluation performance, such as accuracy and precision, using the DLN technique. The system converges after 10 epochs, and the model accuracy

reaches 90.16 percent for TSA and 100 percent for SSA. The model evaluation performance of approach is shown in Table 4 and 5.
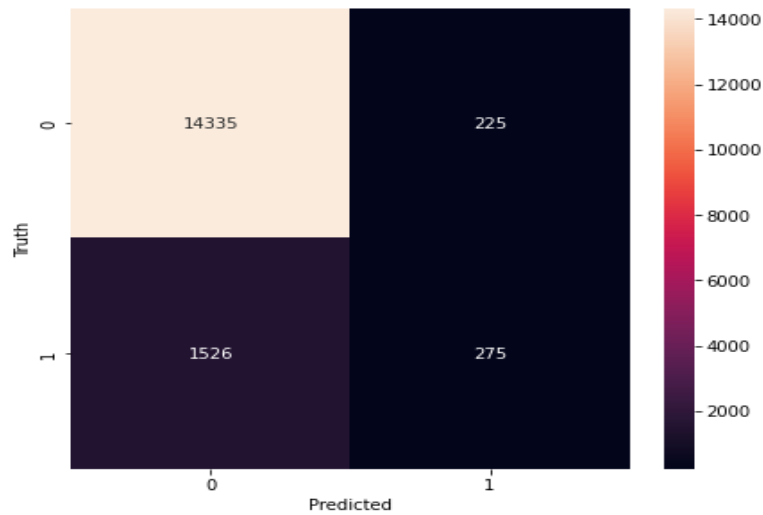

Figure 6: Confusion Matrix for the TSA Developed Model. TP=14335; TN=275; FP=225; FN=1526

Table 4: Evaluation Performance for TSA

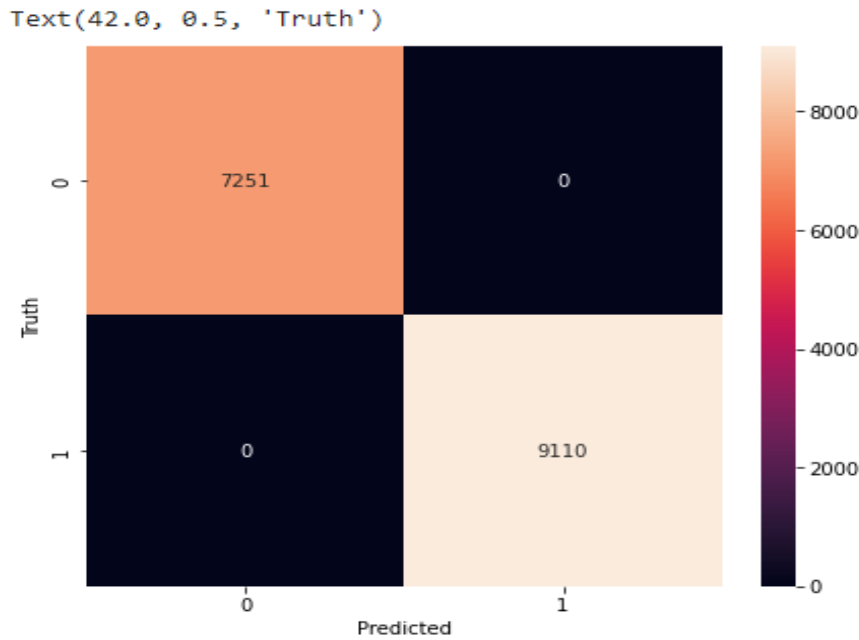| Measure	Evaluation (%)	Derivations
Sensitivity	90.38	TRP=TP/(TP+FN)
Precision	98.45	PPV=TP/(TP+FP)
Accuracy	90.16	ACC+(TP+TN)/(P+N)

Text(42.0, 0.5, 'Truth')

Figure 7: Confusion Matrix for the SSA Developed Model. TP=7251; TN=9110; FP=0; FN=0

Table 5: Evaluation Performance for SSA

Measure	Evaluation (%)	Derivations
Sensitivity	100	TPR=TP/(TP+FN)
Precision	100	PPV=TP/(TP+FP)
Accuracy	100	ACC=(TP+TN)/(P+N)

A. **Compare Results on IEEE 9 Bus System**

This section as shown in Figure 8, showing the modeling of IEEE 9 bus system in DIgSILENT power factory, which is used to verify the evaluation results obtained from TSA and SSA. DIgSILENT is used to run time-domain simulations and eigenvalues computation for these systems. In addition to the oscillation modes, the generator rotor angle, voltage magnitude, active power, and reactive power at all buses are also noted. Additionally, these simulations are performed for 10 seconds with a 0.3 second time difference. Since Neural Network requires so much data to train, therefore, Table 6, shows loaded data for IEEE 9 bus system generated been used for the training and testing, consisting of 62,500 target values. With valid target values of 18,750 testing samples and 43,750 training samples were recovered for the IEEE 9-Bus system. The oscillations displayed by this system have eigenvalues that are consistent with both

local and inter-area modes. For SSA, the simulation revealed substantial eigenvalue errors. In contrast to the TSA, whose LSTM predictions offered straightforward evaluation performance projections, this system's LSTM prediction were precise and closely matched with the dynamics of the simulated oscillatory modes.
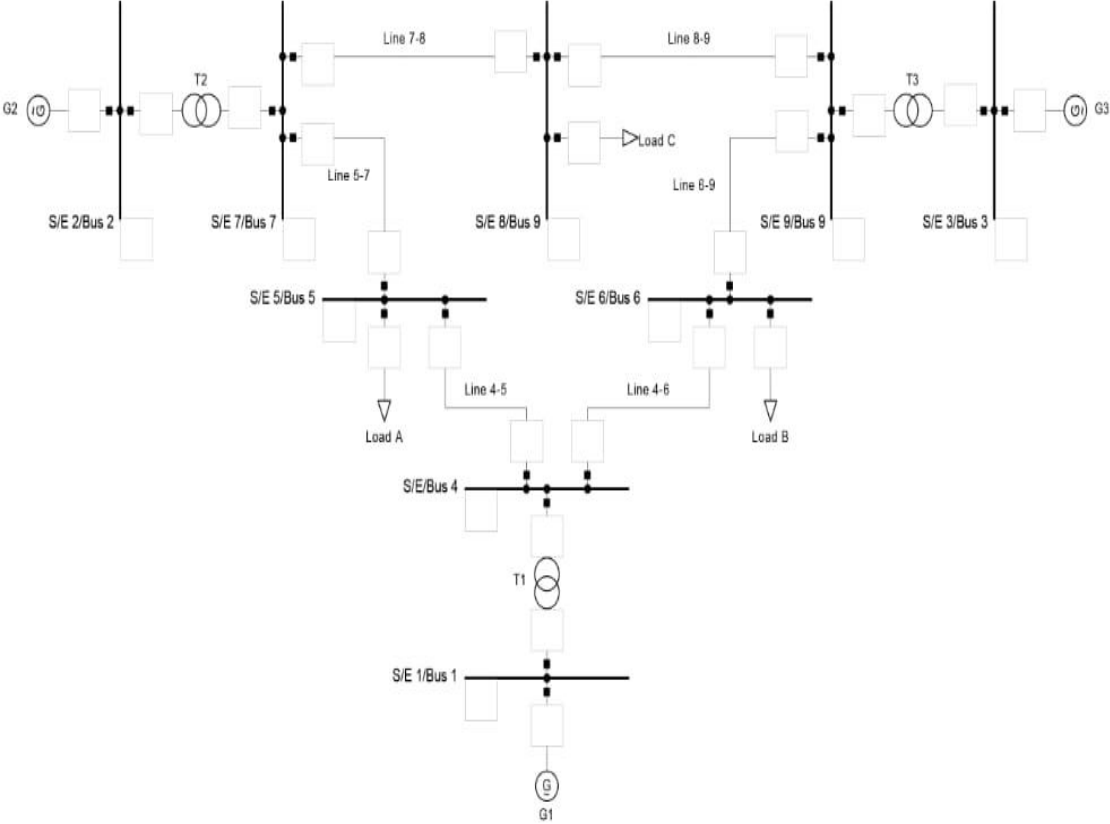

Figure 8: Modelling of IEEE 9 Bus System in DIgSILENT

Table 6: Loaded data for IEEE 9 bus system

V(p.u)	P(KW)	Q (KVAr)	δ(Θ)	TSA Target	SSA Target
0.17958	-123.513	171.9536	-121.034	0	1
0.541271	191.1149	-377.243	26.03689	0	1
0.21862	312.9513	61.45572	172.7484	0	0
0.437684	-202.49	-101.296	-40.9198	0	0.982346655
0.441616	528.1544	-257.218	105.0707	0	0.982346655
0.210953	-162.216	160.9706	-109.329	0	0.10730671
0.542129	238.5471	-392.568	35.91947	0	0.10730671
0.194307	277.8757	75.5049	-179.199	0	0.085283166
0.459572	-195.994	-154.359	-34.6968	0	0.085283166
0.428978	542.6657	-250.911	109.4685	0	0
0.228289	-186.864	148.0511	-106.753	0	0
0.534469	254.3771	-375.392	36.6825	0	0
0.198982	272.5964	83.33363	179.7563	0	0
0.441242	-197.513	-114.59	-37.5489	0	0
0.445292	530.6067	-272.797	104.8101	0	0
0.194562	-150.778	160.4638	-113.223	0	0
0.542532	191.7196	-392.29	28.39765	0	0
0.227462	338.5404	33.06602	169.661	1	0.982346655
0.418274	-235.976	-78.9364	-49.4565	1	0.982346655
0.468614	509.4048	-308.579	91.10054	1	0.10730671

Figure 9 and Table 7 shows, the TSA model confusion matrix used to calculate the created model's evaluation performance, such as accuracy and precision, using the DLNN technique. The confusion matrix TSA developed model results; TP=2300, TN=5900, FP=4000, FN=370. The system converges after 82 epochs, and the model accuracy reaches 65 percent for TSA.
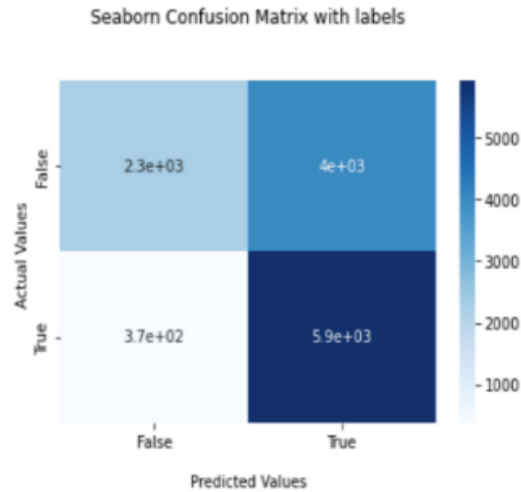
Figure 9: Confusion matrix for the TSA IEEE 9 bus system

Table 7: Evaluation Performance for TSA of IEEE 9 bus system

Measure	Evaluation (%)	Derivations
Sensitivity	94	TPR=TP/(TP+FN)
Precious	86	PPV=TP/(TP+FP)
Accuracy	65	ACC=(TP+TN)/(P+N)

The result obtained for SSA is a Regression approach because the target values have so many floats and less integers. The system converges after 40 epochs, resulting to a Mean Squared Error of 0.183, Root Mean Squared Error 0.4277849927. Figure 10 shows the Residual Distribution Curve in which the prediction is over predicted and under predicted, because most of the value predicted ranges from -0.5 and 0.5

print ('MSE: ' + str(mse))
print ('MSE: ' + str(rmse))
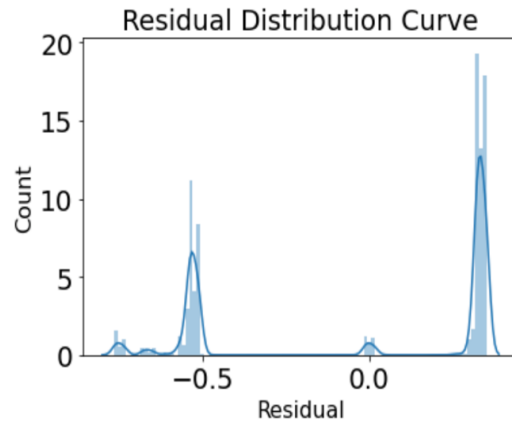print ('Epochs: ' + str(5))
MSE: 0.183
RMSE: 0.4277849927

Figure 10: Residual Distribution Curve

Several works on TSA and SSA were compared to the results by using various machine learning techniques. Table 8 compares the accuracy of various approaches for forecasting TSA and SSA. The suggested method is compared to CNN and LSTM in Table 8 to forecast TSA and SSA, and it is then tested using the IEEE 58, IEEE 60, and New England 39 bus systems. The main comparative metrics are MSE, RMSE, Accuracy, Sensitivity, and Precision. The Nigeria 28 bus system, which uses LSTM to enhance its accuracy, sensitivity, and precision, has faultless assessment performance for both TSA and SSA. The low accuracy in TSA is due to the input data acquired, which included so many floats. Meanwhile, utilizing the IEEE 9 bus system, the evaluation performance for accuracy was 65%. In this situation, random hyperparameter adjustment can be used to increase TSA accuracy, but a longer training period is needed. While in the case of SSA, the MSE may be enhanced by the use of random search hyperparameter adjustment and can also be enhanced through the addition of more LSTM layers to ensure that it will not overfit the data.

Table 8: Comparison of performance with TSA and SSA methods

Related works on (TSA and SSA)	Method	Accuracy (%)	Sensitivity (%)	Precision (%)	MSE	RMSE
Nigeria 28 Bus System (proposed work)	LSTM	90.16 100	90.8 100	98.45 100	_	_
IEEE 9 Bus System (proposed work)	LSTM	65	94	86	0.183	0.42778
IEEE 50 Bus System[7].	CNN and LSTM	98.31	_	_	0.00000016	0.0004
New England 39 Bus System[7].	CNN and LSTM	94.5	_	_	0.00001024	0.0032
IEEE 68 Bus System[7].	CNN and LSTM	97.22	_	_	0.00001681	0.0041

VI. CONCLUSION

The integration of power electronics technology with renewable energy sources has made it easier to turn the current power systems into a new generation of power systems with a high penetration of renewable energy and power electronics. Evaluation of the electrical networks' transient and tiny signal stability is exceedingly challenging as a result of this modification. In contrast to conventional time domain simulation and energy function methods, data-driven TSA with SSA methods establish a relationship between system operational parameters and stability status before determining stability results without the need for a power system's physical model or parameter information. Transient stability and small signal stability are crucial for the secure and reliable operation of electricity networks. In this paper, feature-based deep learning algorithms (LSTM) are introduced for assessing tiny signal stability and transient stability. The study's results will help researchers who are interested in the subject by deepening their comprehension of LSTM in evaluating transitory and small signal stability.

REFERENCES

[1] BIN, Z., & XUE, Y. (2019). A method to extract instantaneous features of low frequency oscillation based on trajectory section eigenvalues.

Journal of Modern Power Systems and Clean Energy, *7*(4), 753–766. https://doi.org/10.1007/s40565-019-0556-z

[2] Lim Zhu Aun, S., Bte Marsadek, M., & K. Ramasamy, A. (2017). Small Signal Stability Analysis of Grid Connected Photovoltaic. *Indonesian Journal of Electrical Engineering and Computer Science*, *6*(3), 553. https://doi.org/10.11591/ijeecs.v6.i3.pp553-562

[3] Liu, X., Ding, C., Wang, Z., & Zhou, P. (2011). Direct method to analyze small signal stability of electric power systems. *Dianli Zidonghua Shebei/Electric Power Automation Equipment*, *31*(7), 1–4.

[4] Nikolaev, N., Dimitrov, K., & Rangelov, Y. (2021). A Comprehensive Review of Small-Signal Stability and Power Oscillation Damping through Photovoltaic Inverters. *Energies*, *14*(21), 7372. https://doi.org/10.3390/en14217372

[5] Prasertwong, K., Mithulananthan, N., & Thakur, D. (2010). Understanding Low-Frequency Oscillation in Power Systems. *The International Journal of Electrical Engineering & Education*, *47*(3), 248–262. https://doi.org/10.7227/IJEEE.47.3.2

[6] Sarajcev, P., Kunac, A., Petrovic, G., & Despalatovic, M. (2022). Artificial Intelligence Techniques for Power System Transient Stability Assessment. *Energies*, *15*(2), 507. https://doi.org/10.3390/en15020507

[7] Syafiq, K. A., Younes,J. I., Mohamed, S. El., Khaled, E. (2020). A Unified Online Deep Learning Prediction Model for Small Signal and Transient Stability. IEE Transactions on Power Systems, 35(6).

[8] Krištof, V., & Mešter, M. (2017). Loss of excitation of synchronous generator. *Journal of Electrical Engineering*, *68*(1),   54–60. https://doi.org/10.1515/jee-2017-0007

[9]   Source: National Control Center (NCC), Power Holding Company of Nigerian,2012. Available at: www.nerc.gov.ng

[10]   Mikolov, T., Joulin, A., Chopra, S., Mathieu, M., & Ranzato, M. 'A. (2015). Learninglonger memory in recurrent neural networks. *3rd International Conference on Learning Representations, ICLR 2015 - Workshop Track Proceedings*.

[11]   Ren, C., Xu, Y., & Zhang, Y. (2018). Post-disturbance Transient stability assessmentof power system towards optimal accuracy-speed trade-off. Protection and control of Modern Power Systems, 3(1), 19. https://doi.org/10.1186/s41601-018-0091-3